nature neuroscience

TECHNICAL REPORT



# Millisecond-timescale, genetically targeted optical control of neural activity

Edward S Boyden[1], Feng Zhang[1], Ernst Bamberg[2,3], Georg Nagel[2,5] & Karl Deisseroth[1,4]

**Temporally precise, noninvasive control of activity in well-defined neuronal populations is a long-sought goal of systems neuroscience. We adapted for this purpose the naturally occurring algal protein Channelrhodopsin-2, a rapidly gated light-sensitive cation channel, by using lentiviral gene delivery in combination with high-speed optical switching to photostimulate mammalian neurons. We demonstrate reliable, millisecond-timescale control of neuronal spiking, as well as control of excitatory and inhibitory synaptic transmission. This technology allows the use of light to alter neural processing at the level of single spikes and synaptic events, yielding a widely applicable tool for neuroscientists and biomedical engineers.**

Neural computation depends on the temporally diverse spiking patterns of different classes of neurons that express unique genetic markers and demonstrate heterogeneous wiring properties within neural networks. Although direct electrical stimulation and recording of neurons in intact brain tissue have provided many insights into the function of circuit subfields (for example, see refs. 1–3), neurons belonging to a specific class are often sparsely embedded within tissue, posing fundamental challenges for resolving the role of particular neuron types in information processing. A high–temporal resolution, noninvasive, genetically based method to control neural activity would enable elucidation of the temporal activity patterns in specific neurons that drive circuit dynamics, plasticity and behavior.

Despite substantial progress made in the analysis of neural network geometry by means of non–cell-type-specific techniques like glutamate uncaging (for example, see refs. 4–7), no tool has yet been invented with the requisite spatiotemporal resolution to probe neural coding at the resolution of single spikes. Furthermore, previous genetically encoded optical methods, although elegant[8–10,11], have allowed control of neuronal activity over timescales of seconds to minutes, perhaps owing to their mechanisms for effecting depolarization. Kinetics roughly a thousand times faster would enable remote control of

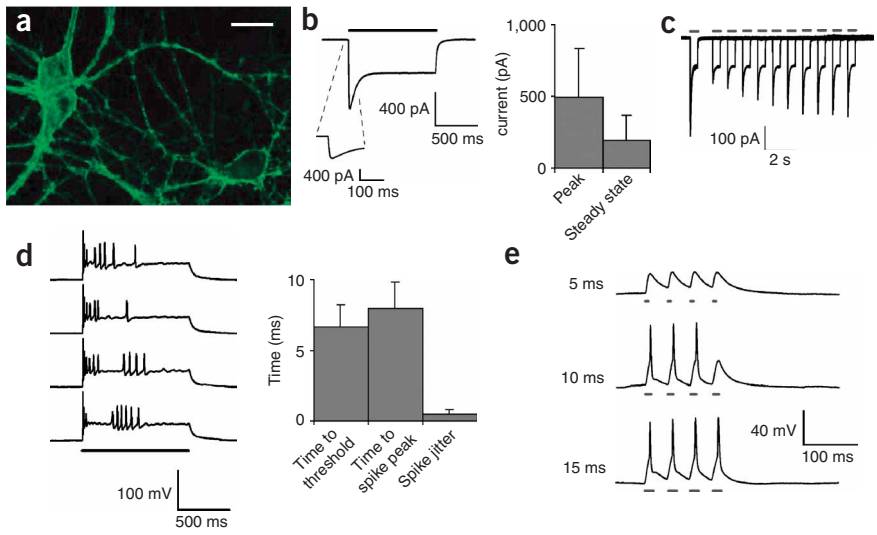


**Figure 1** ChR2 enables light-driven neuron spiking. (**a**) Hippocampal neurons expressing ChR2-YFP (scale bar 30 μm). (**b**) Left, inward current in voltage-clamped neuron evoked by 1 s of GFP-wavelength light (indicated by black bar); right, population data (right; mean ± s.d. plotted throughout; $n = 18$). Inset, expanded initial phase of the current transient. (**c**) Ten overlaid current traces recorded from a hippocampal neuron illuminated with pairs of 0.5-s light pulses (indicated by gray bars), separated by intervals varying from 1 to 10 s. (**d**) Voltage traces showing membrane depolarization and spikes in a current-clamped hippocampal neuron (left) evoked by 1-s periods of light (gray bar). Right, properties of the first spike elicited ($n = 10$): latency to spike threshold, latency to spike peak, and jitter of spike time. (**e**) Voltage traces in response to brief light pulse series, with light pulses (gray bars) lasting 5 ms (top), 10 ms (middle) or 15 ms (bottom).

[1]Department of Bioengineering, Stanford University, 318 Campus Drive West, Stanford, California 94305, USA. [2]Max-Planck-Institute of Biophysics, Department of Biophysical Chemistry, Max-von-Laue-Str. 3, D-60438 Frankfurt am Main, Germany. [3]Department of Biochemistry, Chemistry and Pharmaceutics, University of Frankfurt, Marie-Curie-Str. 9, 60439 Frankfurt am Main, Germany. [4]Department of Psychiatry and Behavioral Sciences, Stanford School of Medicine, 401 Quarry Road, Stanford, California 94305, USA. [5]Present address: Julius-von-Sachs-Institut, University of Würzburg, Julius-von-Sachs-Platz 2–4, D-97082 Würzburg, Germany. Correspondence should be addressed to K.D. (deissero@stanford.edu).

Published online 14 August 2005; doi:10.1038/nn1525

individual spikes or synaptic events. We have therefore devised a new strategy using a single-component ion channel with submillisecond opening kinetics, to enable genetically targeted photostimulation with fine temporal resolution.

Two rhodopsins in the unicellular green alga *Chlamydomonas reinhardtii* were recently identified independently by three groups[12–15]. One of them is a light-gated proton channel (Channelrhodopsin-1; ref. 13), whereas the other, Channelrhododopsin-2 (ChR2), is a light-gated cation channel[12]. The N-terminal 315 amino acids of ChR2 are homologous to the seven-transmembrane structure of many microbial-type rhodopsins; they compose a channel with light-gated conductance (as proposed earlier[16]). Inward currents in ChR2-expressing cells could be evoked within 50 μs after a flash of blue light in the presence of all-*trans* retinal[12], suggesting the possibility that ultrafast neuronal stimulation might be possible with equipment commonly used for visualizing green fluorescent protein (GFP). ChR2 therefore combines some of the best features of previous photostimulation methods, including the speed of a monolithic ion channel[9], and the efficacy of natural light-transduction machinery[11].

We found that ChR2 could be expressed stably and safely in mammalian neurons and could drive neuronal depolarization. When activated with a series of brief pulses of light, ChR2 could reliably mediate defined trains of spikes or synaptic events with millisecond-timescale temporal resolution. This technology thus brings optical control to the temporal regime occupied by the fundamental building blocks of neural computation.

## RESULTS

### Rapid kinetics of ChR2 enables driving of single spikes

To obtain stable and reliable ChR2 expression for coupling light to neuronal depolarization, we constructed lentiviruses containing a ChR2-yellow fluorescent protein (YFP) fusion protein for genetic modification of neurons. Infection of cultured rat CA3/CA1 neurons led to membrane-localized expression of ChR2 for weeks after infection (**Fig. 1a**). Illumination of ChR2-positive neurons with blue light (bandwidth 450–490 nm via Chroma excitation filter HQ470/40×; 300-W xenon lamp) induced rapid depolarizing currents, which reached a maximal rise rate of 160 ± 111 pA/ms within 2.3 ± 1.1 ms after light pulse onset (mean ± s.d. reported throughout paper, $n = 18$; **Fig. 1b**, left). Mean whole-cell inward currents were large: 496 pA ± 336 pA at peak and 193 pA ± 177 pA at steady-state (**Fig. 1b**, right). Light-evoked responses were never seen in cells expressing YFP alone (data not shown). Consistent with the known excitation spectrum of ChR2 (ref. 12), illumination of ChR2-expressing neurons with YFP-spectrum light in the bandwidth 490–510 nm (300-W xenon lamp filtered with Chroma excitation filter HQ500/20×) resulted in currents that were smaller (by 42% ± 20%) than those evoked with the GFP filters. Despite the inactivation of ChR2 with sustained light exposure (**Fig. 1b** and ref. 12), we observed rapid recovery of peak ChR2 photocurrents in neurons (**Fig. 1c**; recovery $\tau = 5.1 \pm 1.4$ s; recovery trajectory fit with Levenberg-Marquardt algorithm; $n = 9$). This rapid recovery is consistent with the well-known stability of the Schiff base (the lysine in transmembrane helix seven, which binds retinal) in microbial-type rhodopsins, and the ability of retinal to re-isomerize to the all-*trans* ground state in a dark reaction, without the need for other enzymes. Light-evoked current amplitudes remained unchanged in patch-clamped neurons during 1 h of pulsed light exposure (data not shown). Thus ChR2 was able to sustainably mediate large-amplitude photocurrents with rapid activation kinetics.

We next examined whether ChR2 could drive spiking of neurons held in current-clamp mode, with the same steady illumination protocol we used for eliciting ChR2-induced currents (**Fig. 1d**, left). Early in an epoch of steady illumination, single neuronal spikes were rapidly and reliably elicited (8.0 ± 1.9 ms latency to spike peak, $n = 10$; **Fig. 1d**, right), consistent with the fast rise times of ChR2 currents described above. However, any subsequent spikes elicited during steady illumination were poorly timed (**Fig. 1d**, left). Thus, steady illumination is not adequate for controlling the timing of ongoing spikes with ChR2, despite the reliability of the first spike. Earlier patch-clamp studies using somatic current injection showed that spike times were more reliable during periods of rapidly rising membrane potential than during periods of steady high-magnitude current injection[17]. This is consistent with our finding that steady illumination evoked a single reliably timed spike, followed by irregular spiking.

In searching for a strategy to elicit precisely timed series of spikes with ChR2, we noted that the single spike reliably elicited by steady

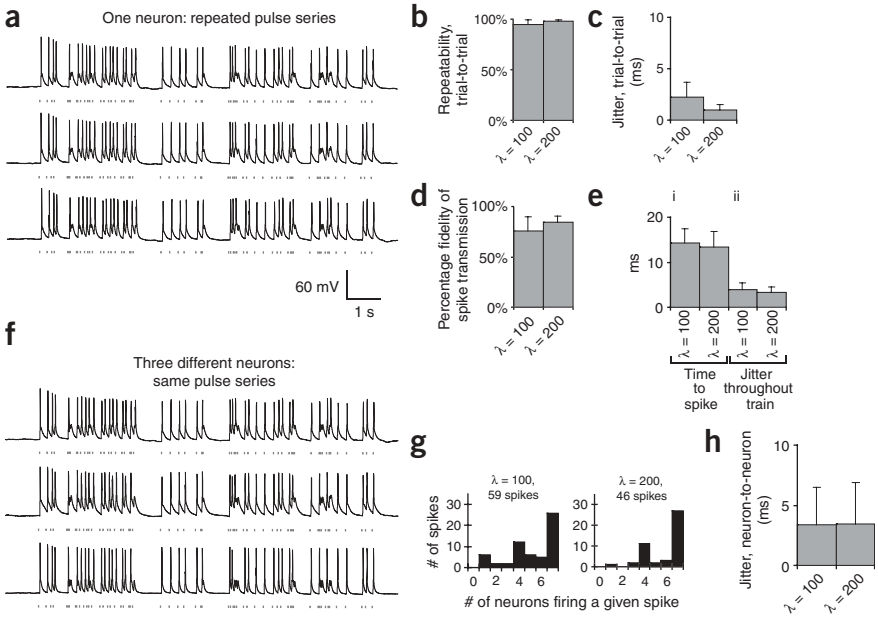


**Figure 2** Realistic spike trains driven by series of light pulses. (**a**) Voltage traces showing spikes in a single current-clamped hippocampal neuron, in response to three deliveries of a Poisson train (with mean interval $\lambda = 100$ ms) of light pulses (gray dashes). (**b**) Trial-to-trial repeatability of light-evoked spike trains, as measured by comparing the presence or absence of a spike in two repeated trials of a Poisson train (either $\lambda = 100$ ms or $\lambda = 200$ ms) delivered to the same neuron ($n = 7$ neurons). (**c**) Trial-to-trial jitter of spikes, across repeated light-evoked spike trains. (**d**) Percent fidelity of spike transmission throughout entire 8-s light pulse series. (**e**) Latency of spikes throughout each light pulse series (i) and jitter of spike times throughout train (ii). (**f**) Voltage traces showing spikes in three different hippocampal neurons, in response to the same temporally patterned light stimulus (gray dashes) used in **a**. (**g**) Histogram showing how many of the seven neurons spiked in response to each light pulse in the Poisson train. (**h**) Neuron-to-neuron jitter of spikes evoked by light stimulation.

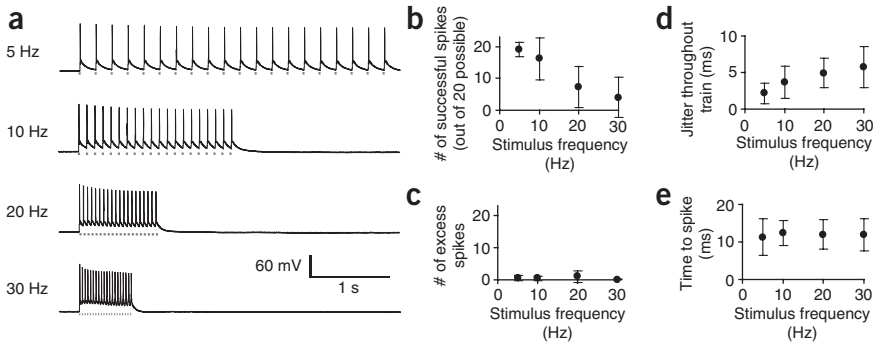


**Figure 3** Frequency dependence of coupling between light input and spike output. (**a**) Voltage traces showing spikes in a current-clamped hippocampal neuron evoked by 5-, 10-, 20- or 30-Hz trains of light pulses (gray dashes). (**b**) Population data showing the number of spikes (out of 20 possible) evoked in current-clamped hippocampal neurons. (**c**) Number of extraneous spikes evoked by the trains of light pulses, for the experiment described in **b**. (**d**) Jitter of spike times throughout the train of light pulses for the experiment described in **b**. (**e**) Latency to spike peak throughout the light pulse train for the experiment described in **b**.



illumination had extremely low temporal jitter from trial to trial, as reflected by the small standard deviation of the spike times across trials (**Fig. 1d**, right; 0.5 ± 0.3 ms, average of $n = 10$ neurons). This observation led us to devise a pulsed-light strategy that would take advantage of the low jitter of the single reliable spike evoked at light pulse onset. In order for this to work, the conductance and kinetics of ChR2 would have to permit peak currents of sufficient amplitude to reach spike threshold, during a light pulse of duration shorter than the desired interspike interval. We found that multiple pulses of light with interspersed periods of darkness could elicit trains of multiple spikes (**Fig. 1e**; shown for a 25-Hz series of four pulses). Longer light pulses evoked single spikes with greater probability than short light pulses (**Fig. 1e**). In the experiments described here, we used light pulse durations of 5, 10 or 15 ms. Thirteen high-expressing neurons fired reliable spikes, and five low-expressing neurons could reliably be depolarized to subthreshold levels. The ability to easily alter light pulse duration suggests that a straightforward method for eliciting spikes, even in multiple neurons having different ChR2 current densities, would involve titrating the light pulse duration until single spikes were reliably obtained in all the neurons being illuminated. Modulation of light intensity would also allow for this kind of control.

## Precise spike trains elicited by series of light pulses

The precise control described above raised the prospect of generating arbitrary spike patterns, even mimicking natural neural activity. To test this possibility, we generated series of light pulses, the timings of which were selected according to a Poisson distribution, commonly used to model natural spiking. A single hippocampal neuron could fire repeatable spike trains in response to multiple deliveries of the same Poisson-distributed series of light pulses (**Fig. 2a**; response to a repeated 59-pulse-long series of light pulses, with each pulse of 10-ms duration, and with mean interpulse interval of $\lambda = 100$ ms). These optically driven spike trains were very consistent across repeated deliveries of the same series of light pulses: on average, >95% of the light pulses in a series elicited spikes during one trial if and only if they elicited spikes on a second trial, for both the $\lambda = 100$ ms series (**Fig. 2a**) and a second series (mean interval $\lambda = 200$ ms) comprising 46 spikes (**Fig. 2b**; $n = 7$ neurons). We increased light pulse duration until reliable spiking was obtained: we used trains of 10-ms light pulses for four of the seven neurons and trains of 15-ms light pulses for the other three (for the analyses of **Fig. 2**, all data were pooled). The trial-to-trial jitter for each individual spike was very small across repeated deliveries of the same Poisson series of light pulses (on average, 2.3 ± 1.4 ms and 1.0 ± 0.5 ms for $\lambda = 100$ ms and $\lambda = 200$ ms, respectively; **Fig. 2c**). Throughout a series of pulses, the efficacy of eliciting spikes throughout the train was maintained (76% and 85% percent of light pulses successfully evoked spikes, respectively; **Fig. 2d**), with small latencies (**Fig. 2e**). As another indication of how precisely spikes can be elicited throughout an entire series of pulses, we measured the standard deviation of the latencies of each spike across all the spikes in the train. This 'throughout-train' spike jitter was quite small (3.9 ± 1.4 ms and 3.3 ± 1.2 ms; **Fig. 2e**), despite presumptive channel inactivation during the delivery of a series of pulses. Hence, pulsed optical activation of ChR2 elicits precise, repeatable spike trains in a single neuron, over time.

Even in different neurons, the same precise spike train could be elicited by a particular series of light pulses (shown for three hippocampal neurons in **Fig. 2f**). Although the large heterogeneity of different neurons—for example, in their membrane capacitance (68.8 ± 22.6 pF) and resistance (178.8 ± 94.8 MΩ)—might be expected to introduce significant variability in their electrical responses to photostimulation, the strong nonlinearity of light-spike coupling dominated this variability. Indeed, different neurons responded in similar ways to a given light pulse series, with 80–90% of the light pulses in a series eliciting spikes in at least half the neurons examined (**Fig. 2g**). To quantitatively compare the reliability of spike elicitation in different neurons, for each pulse, we calculated the standard deviation of spike latencies (jitter) across all the neurons. Remarkably, this across-neuron jitter (3.4 ± 1.0 ms and 3.4 ± 1.2 ms for the pulses in the $\lambda = 100$ ms and $\lambda = 200$ ms trains, respectively; **Fig. 2h**) was similar to the within-neuron jitter measured throughout the light pulse series (**Fig. 2e**). Thus, heterogeneous populations of neurons can be controlled in concert, with practically the same precision observed for the control of single neurons over time.

Having established the ability of ChR2 to drive sustained naturalistic trains of spikes, we next probed the frequency response of light-spike coupling. ChR2 enabled driving of spike trains from 5 to 30 Hz (**Fig. 3a**; here tested with series of twenty 10-ms light pulses). It was easier to evoke more spikes at lower frequencies than at higher frequencies (**Fig. 3b**; $n = 13$ neurons). Light pulses delivered at 5 or 10 Hz could elicit long spike trains (**Fig. 3b**), with spike probability dropping off at higher frequencies of stimulation. For these experiments, the light pulses used were 5 ms ($n = 1$), 10 ms ($n = 9$) or 15 ms ($n = 3$) in duration (data from all 13 cells were pooled for the population analyses of **Fig. 3**). As expected from the observation that light pulses generally elicited single spikes (**Figs. 1d** and **2**), almost no extraneous spikes occurred during the delivery of trains of light pulses (**Fig. 3c**). Even at higher frequencies, the throughout-train temporal jitter of spike timing remained very low (typically <5 ms; **Fig. 3d**) and the latency to spike remained constant across frequencies (~10 ms throughout; **Fig. 3e**). Thus ChR2 can mediate spiking across a physiologically relevant range of firing frequencies.

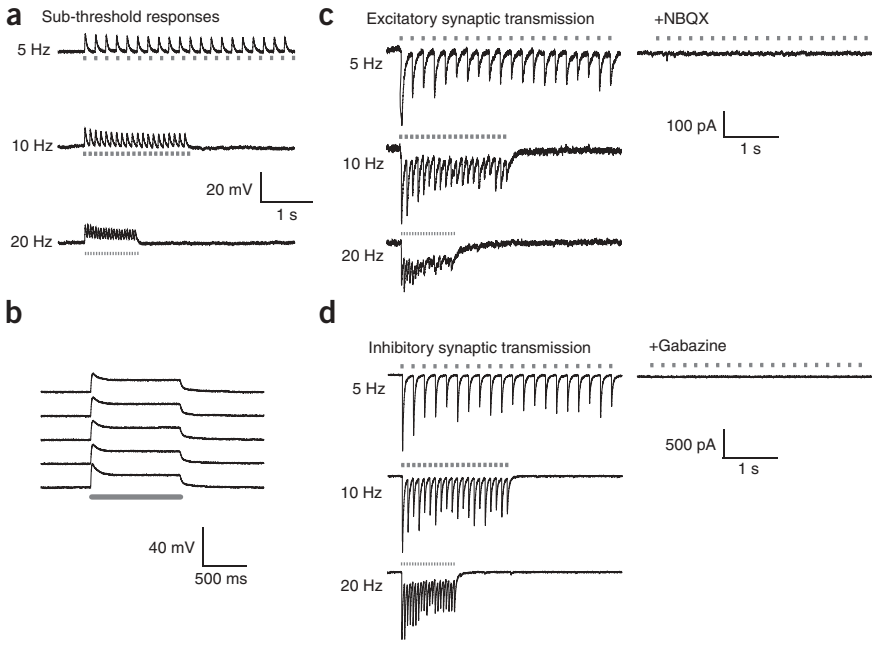


**Figure 4** Simulated and natural synaptic transmission evoked via ChR2. (**a**) Voltage traces showing trains of subthreshold depolarizations in a current-clamped hippocampal neuron in response to trains of light pulses (gray dashes). (**b**) Repeated light pulses induced reliable depolarizations. (**c**) Excitatory synaptic transmission driven by light pulses. The selective glutamatergic transmission blocker NBQX abolished these synaptic responses (right). (**d**) Inhibitory synaptic transmission driven by light pulses. The selective GABAergic transmission blocker gabazine abolished these synaptic responses (right).

## Remote activation of subthreshold and synaptic responses

For many cellular and systems neuroscience processes (and for nonspiking neurons in species like *Caenorhabditis elegans*) subthreshold depolarizations convey physiologically significant information. For example, subthreshold depolarizations are potent for activating synapse-to-nucleus signaling[18], and the relative timing of subthreshold and suprathreshold depolarizations can determine the direction of synaptic plasticity[19]. But compared with driving spiking, it is in principle more difficult to drive reliable and precisely sized subthreshold depolarizations. The sharp threshold for action potential production facilitates reliable ChR2-induced spiking, and the all-or-none dynamics of spiking produces virtually identical waveforms from spike to spike (as seen throughout **Figs. 1–3**), even in the presence of significant neuron-to-neuron variability in electrical properties. In contrast, subthreshold depolarizations, which operate in a more linear regime of membrane voltage, will lack these intrinsic normalizing mechanisms. Nevertheless, subthreshold depolarizations evoked by repeated light pulses were reliably evoked over a range of frequencies (**Fig. 4a**), with spaced repeated depolarizations resulting in a coefficient of variation of 0.06 ± 0.03 (**Fig. 4b**; $n = 5$). Thus, ChR2 can be used to drive subthreshold depolarizations of reliable amplitude.

Finally, synaptic transmission was also easily controlled with ChR2. Indeed, both excitatory (**Fig. 4c**) and inhibitory (**Fig. 4d**) synaptic events could be evoked in ChR2-negative neurons receiving synaptic input from ChR2-expressing neurons.

## Expression of ChR2 has minimal side effects

We conducted extensive controls to test whether simply expressing ChR2 would alter the electrical properties or survival of neurons. Lentiviral expression of ChR2 for at least 1 week did not alter neuronal membrane resistance (212 ± 115 MΩ for ChR2$^+$ cells versus 239.3 ± 113 MΩ for ChR2$^-$ cells; **Fig. 5a**; $P > 0.45$; $n = 18$ each) or resting potential (−60.6 ± 9.0 mV for ChR2$^+$ cells versus −59.4 ± 6.0 mV for ChR2$^-$ cells; **Fig. 5b**; $P > 0.60$), when measured in the absence of light. This suggests that in neurons, ChR2 has little basal electrical activity or passive current-shunting ability. It also suggests that expression of ChR2 did not compromise cell health, as indicated by electrical measurement of membrane integrity. As an independent measure of cell health, we stained live neurons with the membrane-impermeant DNA-binding dye propidium iodide. ChR2 expression did not affect the percentage of neurons that took up propidium iodide (1/56 ChR2$^+$ neurons versus 1/49 ChR2$^-$ neurons; $P > 0.9$ by $\chi^2$ test). Neither did we see pyknotic nuclei, indicative of apoptotic degeneration, in cells expressing ChR2 (data not shown). We also checked for alterations in the dynamic electrical properties of neurons. In darkness, there was no difference in the voltage change resulting from 100 pA of injected current, in either the hyperpolarizing (−22.6 ± 8.9 mV for ChR2$^+$ neurons versus −24.5 ± 8.7 mV for ChR2$^-$ neurons; $P > 0.50$) or depolarizing (+18.9 ± 4.4 mV for ChR2$^+$ versus 18.7 ± 5.2 mV for ChR2$^-$ neurons; $P > 0.90$) directions. Nor was there any difference in the number of spikes evoked by a 0.5-s current injection of +300 pA (6.6 ± 4.8 for ChR2$^+$ neurons versus 5.8 ± 3.5 for ChR2$^-$ neurons; **Fig. 5c**; $P > 0.55$). Thus, ChR2 does not significantly jeopardize cell health or basal electrical properties of the expressing neuron.

We also measured the electrical properties described above, 24 h after exposing ChR2$^+$ neurons to a typical light pulse protocol (1 s of 20-Hz 15-ms light flashes, once per minute, for 10 min). Neurons expressing ChR2 and exposed to light had basal electrical properties similar to non-flashed ChR2$^+$ neurons: cells had normal membrane resistance (178 ± 81 MΩ; **Fig. 5a**; $P > 0.35$; $n = 12$ and resting potential (−59.7 ± 7.0 mV; **Fig. 5b**; $P > 0.75$). Exposure to light also did not predispose neurons to cell death, as measured by live-cell propidium iodide uptake (2/75 ChR2+ neurons versus 3/70 ChR2- neurons; $P > 0.55$ by $\chi^2$ test). Finally, neurons expressing ChR2 and exposed to light also had normal spike counts elicited from somatic current injection (6.1 ± 3.9; **Fig. 5c**; $P > 0.75$). Thus, membrane integrity, cell health and electrical properties were normal in neurons expressing ChR2 and exposed to light.

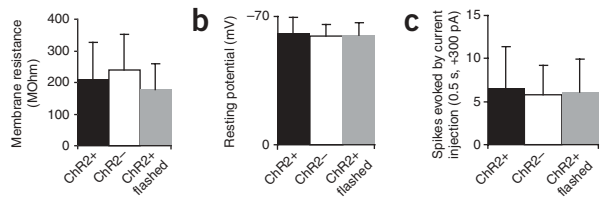


**Figure 5** Basal and dynamic electrical properties of neurons expressing ChR2. (**a**) Membrane resistance of neurons expressing ChR2 (black; $n = 18$), not expressing ChR2 (white; $n = 18$) or expressing ChR2 and measured 24 h after exposure to a typical light-pulse protocol (gray; $n = 12$). (**b**) Membrane resting potential of the same neurons described in **a**. (**c**) Number of spikes evoked by a 300-pA depolarization of the same neurons described in **a**.

## DISCUSSION

Combining the best aspects of earlier approaches that use light to drive neural circuitry, the technology described here demonstrates voltage control significantly faster than previous genetically encoded photostimulation methods[8–11]. Notably, the ChR2 method does not rely on synthetic chemical substrates or genetic orthogonality of the transgene and the host organism. Although the ChR2 molecule does require the cofactor all-*trans* retinal for light transduction[12], no all-*trans* retinal was added either to the culture medium or recording solution for any of the experiments described here. Background levels of retinal may be sufficient in many cases; moreover, the commonly used culture medium supplement B-27 used here (see Methods) includes retinyl acetate, and additional supplementation with all-*trans* retinal or its precursors may assist in the application of ChR2 to the study of neural circuits in various tissue environments.

We used pulsed light delivery to take full advantage of the fast kinetics and high conductance of ChR2. This strategy was made possible with fast optical switches, but other increasingly common equipment, such as pulsed lasers, would also suffice. Unlike electrical stimulation, glutamate uncaging[20–22] and high-powered laser excitation methods[23], ChR2 can be genetically targeted to allow probing of specific neuron subclasses within a heterogeneous neural circuit, avoiding fibers of passage and the simultaneous stimulation of multiple cell types.

Because ChR2 is encoded by a single open reading frame of only 315 amino acids, it is feasible to express ChR2 in specific subpopulations of neurons in the nervous system through genetic methods including lentiviral vectors (as we have done) and in transgenic mice, thus permitting the study of the function of individual types of neurons in intact neural circuits and even *in vivo*. Cell-specific promoters will allow targeting of ChR2 to various well-defined neuronal subtypes, which will permit future exploration of their causal function in driving downstream neural activity (measured using electrophysiological and optical techniques) and animal behavior. ChR2 also could be used to resolve functional connectivity of particular neurons or neuron classes in intact circuits in response to naturalistic spike trains (**Fig. 2**) or rhythmic activity (**Fig. 3**), for example, by using acute slice preparations after intracranial viral injections.

Recent papers have explored the topics of static and dynamic microcircuit connectivity using calcium imaging of spontaneous activity[24], multi-neuron patch-clamping[25,26] and glutamate uncaging[6]. These studies have reported surprisingly refined and precise connections between neurons. However, finer-scale dissection of microcircuits, at the level of molecularly defined neuron classes (such as cannabinoid receptor–expressing cortical neurons, parvalbumin-positive interneurons or cholinergic modulatory neurons) would be greatly facilitated through use of a genetically targeted, temporally precise tool like ChR2. This holds true also for recent microstimulation experiments that have demonstrated profound influences of a cluster of neurons in controlling attention, decision making or action[2,3,27,28]. Understanding precisely which cell types contribute to these functions could provide great insight into how they are computed at the circuit level. Because the light power required for ChR2 activation (8–12 mW/mm$^2$) is fairly low, it is possible that ChR2 will be an effective tool for *in vivo* studies of circuit maps and behavior, even in mammals. Finally, the efficacious and safe transduction of light with a single natural biological component also could serve biotechnological needs, in high-throughput studies of activity-dependent signal transduction and gene expression programs, for example, in guiding stem cell differentiation[29] and screening for drugs that modulate neuronal responses to depolarization. Thus, the technology described here may fulfill the long-sought goal of a method for noninvasive, genetically targeted, temporally precise control of neuronal activity, with potential applications ranging from neuroscience to biomedical engineering.

## METHODS

**Plasmid constructs.** The ChR2-YFP gene was constructed by in-frame fusing EYFP (Clontech) to the C terminus of the first 315 amino acid residues of ChR2 (GenBank accession number AF461397) via a *Not*I site. The lentiviral vector pLECYT was generated by PCR amplification of ChR2-YFP with primers 5′-GGCAGCGCTGCCACCATGGATTATGGAGGCGCCCTGAGT-3′ and 5′-GGCACTAGTCTATTACTTGTACAGCTCGTC-3′ and ligation into pLET (gift from E. Wexler and T. Palmer, Stanford University) via the *Afe*I and *Spe*I restriction sites. The plasmid was amplified and then purified using MaxiPrep kits (Qiagen).

**Viral production.** VSVg pseudotyped lentiviruses were produced by triple transfection of 293FT cells (Invitrogen) with pLECYT, pMD.G and pCMVΔR8.7 (gifts from E. Wexler and T. Palmer) using Lipofectamine 2000. The lentiviral production protocol is the same as previously described[30] except for the use of Lipofectamine 2000 instead of calcium phosphate precipitation. After harvest, viruses were concentrated by centrifuging in a SW28 rotor (Beckman Coulter) at 20,000 rpm for 2 h at 4 °C. The concentrated viral titer was determined by FACS to be between $5 \times 10^8$ and $1 \times 10^9$ infectious units (IU) per ml.

**Hippocampal cell culture.** Hippocampi of postnatal day 0 (P0) Sprague-Dawley rats (Charles River) were removed and treated with papain (20 U/ml) for 45 min at 37 °C. The digestion was stopped with 10 ml of MEM/Earle salts without L-glutamine along with 20 mM glucose, Serum Extender (1:1000), and 10% heat-inactivated fetal bovine serum containing 25 mg of bovine serum albumin (BSA) and 25 mg of trypsin inhibitor. The tissue was triturated in a small volume of this solution with a fire-polished Pasteur pipette, and ~100,000 cells in 1 ml plated per coverslip in 24-well plates. Glass coverslips (prewashed overnight in HCl followed by several 100% ethanol washes and flame sterilization) were coated overnight at 37 °C with 1:50 Matrigel (Collaborative Biomedical). Cells were plated in culture medium: Neurobasal containing 2× B-27 (Life Technologies) and 2 mM Glutamax-I (Life Technologies). The culture medium supplement B-27 contains retinyl acetate, but no B-27 was present during recording and no all-*trans* retinal was added to the culture medium or recording medium for any of the experiments described. One-half of the medium was replaced with culture medium the next day, giving a final serum concentration of 1.75%.

**Viral infection.** Hippocampal cultures were infected on day 7 *in vitro* (DIV 7) using fivefold serial dilutions of lentivirus (~$1 \times 10^6$ IU/ml). Viral dilutions were added to hippocampal cultures seeded on coverslips in 24-well plates and then incubated at 37 °C for 7 d before experimentation.

**Confocal imaging.** Images were acquired on a Leica TCS-SP2 LSM confocal microscope using a 63× water-immersion lens. Cells expressing ChR2-YFP were imaged live using YFP microscope settings, in Tyrode solution containing (in mM) NaCl 125, KCl 2, $CaCl_2$ 3, $MgCl_2$ 1, glucose 30 and HEPES 25 (pH 7.3 with NaOH).

Propidium iodide (Molecular Probes) staining was carried out on live cells by adding 5 μg/ml propidium iodide to the culture medium for 5 min at 37 °C, washing twice with Tyrode solution and then immediately counting the number of ChR2$^+$ and ChR2$^-$ cells that took up propidium iodide. Coverslips were then fixed for 5 min in PBS + 4% paraformaldehyde, permeabilized for 2 min with 0.1% Triton X-100 and then immersed for 5 min in PBS containing 5 μg/ml propidium iodide for detection of pyknotic nuclei. At least eight fields of view were examined per coverslip.

**Electrophysiology and optical methods.** Cultured hippocampal neurons were recorded at approximately DIV 14 (7 d post-infection). Neurons were recorded by means of whole-cell patch clamp, using Axon Multiclamp 700B (Axon Instruments) amplifiers on an Olympus IX71 inverted scope equipped with a 20× objective lens. Borosilicate glass (Warner) pipette resistances were ~4 MΩ, range 3–8 MΩ. Access resistance was 10–30 MΩ and was monitored throughout the recording. Intracellular solution consisted of (in mM) 97

potassium gluconate, 38 KCl, 0.35 EGTA, 20 HEPES, 4 magnesium ATP, 0.35 sodium GTP, 6 NaCl, and 7 phosphocreatine (pH 7.25 with KOH). Neurons were recorded in Tyrode solution (above). All experiments were performed at room temperature (22–24 °C). For all experiments except for the synaptic transmission data shown in **Figure 4b,c**, we patched fluorescent cells immersed in Tyrode solution containing 5 μM NBQX and 20 μM gabazine to block synaptic transmission.

Photocurrents were measured while holding neurons in voltage clamp at −65 mV. Recovery from inactivation was measured by measuring photocurrents while illuminating neurons with pairs of 500-ms duration light pulses, separated by periods of darkness lasting 1–10 s.

Spiking was measured while injecting current to keep the voltage of the cell at approximately −65 mV (holding current ranging from 0 pA to −200 pA). For synaptic transmission experiments, we patched nonfluorescent neurons near ChR2-expressing neurons, immersed in Tyrode solution containing either 20 μM gabazine to isolate the excitatory postsynaptic response or in 5 μM NBQX to isolate the inhibitory postsynaptic response. To confirm whether the evoked potentials were indeed synaptically driven, after photostimulation, we blocked all postsynaptic receptors with solution containing both 20 μM gabazine and 5 μM NBQX and carried out photostimulation again.

pClamp 9 software (Axon Instruments) was used to record all data, and a DG-4 high-speed optical switch with 300-W xenon lamp (Sutter Instruments) was used to deliver the light pulses for ChR2 activation. An Endow GFP filter set (excitation filter HQ470/40×, dichroic Q495LP; Chroma) was used for delivering blue light for ChR2 activation. YFP was visualized with a standard YFP filter set (excitation HQ500/20×, dichroic Q515LP, emission HQ535/30 m; Chroma). Through a 20× objective lens, power density of the blue light was 8–12 mW/mm$^2$, measured with a power meter (Newport).

Pulse series were synthesized by custom software written in MATLAB (MathWorks) and then exported through pClamp 9 via a Digidata board (Axon) attached to a PC. Poisson trains were generated in MATLAB by creating series of pulses with inter-pulse intervals independently picked from a Poisson distribution with mean λ. Poisson trains were 8 s long, with mean interval λ = 100 or 200 ms. For biophysical realism, a 10-ms minimum refractory period was enforced between consecutive light pulses.

Membrane resistance was measured in voltage clamp mode with 20-mV depolarizing steps lasting 75 ms. Spike rates due to direct current injection were measured with 300-pA current steps lasting 0.5 s.

**Data analysis.** Data was analyzed using Clampfit (Axon) and custom software written in MATLAB. Spikes were extracted by looking for voltage crossings of a threshold (typically 60 mV above resting potential), and latencies were measured from the onset of the light pulse to the spike peak. Extraneous spikes were measured as the number of extra spikes after a single light pulse, plus any spikes occurring later than 30 ms after the onset of a light pulse.

Jitter was calculated as the standard deviation of spike latencies, measured either across all the spikes throughout a spike train ('throughout-train' jitter), or for a particular spike across different trains (when gauging trial-to-trial reliability, or across different neurons). For display of population data, throughout-train jitter and trial-to-trial jitter were averaged across all neurons, and neuron-to-neuron jitter was averaged across all spikes. For all jitter analyses, light pulses which failed to elicit a spike were ignored. For the across-neuron jitter analysis shown in **Figure 2h**, light pulses that did not elicit spikes in all seven neurons were ignored (leaving 31/59 light pulses for the λ = 100 ms stimulus, and 30/46 light pulses for the λ = 200 ms stimulus).

**ACKNOWLEDGMENTS**

We would like to thank L. Meltzer and N. Adeishvili for experimental assistance; C. Niell, C. Chan and J.P. Levy for helpful discussions and D. Ollig for technical help. E.B. and G.N. are supported by the Max-Planck-Society and acknowledge a grant from the German Research Foundation (DFG) in the research unit 472 (Molekulare Bioenergetik). E.S.B. is supported by the Helen Hay Whitney Foundation, the Dan David Prize Foundation, and National Institute on Deafness and Other Communication Disorders, and F.Z. is supported by a US National Institutes of Health predoctoral fellowship. K.D. is supported by the National Institute of Mental Health, the Stanford Department of Bioengineering, the Stanford Department of Psychiatry and Behavioral Sciences, the Neuroscience Institute at Stanford, the National Alliance for Research On Schizophrenia and Depression and the Culpeper, Klingenstein, Whitehall, McKnight, and Albert Yu and Mary Bechmann Foundations.

**COMPETING INTERESTS STATEMENT**

The authors declare that they have no competing financial interests.

Received 12 May; accepted 26 July 2005
Published online at http://www.nature.com/natureneuroscience/



1. Kandel, E.R., Spencer, W.A. & Brinley, F.J., Jr. Electrophysiology of hippocampal neurons. I. Sequential invasion and synaptic organization. *J. Neurophysiol.* **24**, 225–242 (1961).
2. Ditterich, J., Mazurek, M.E. & Shadlen, M.N. Microstimulation of visual cortex affects the speed of perceptual decisions. *Nat. Neurosci.* **6**, 891–898 (2003).
3. Salzman, C.D., Britten, K.H. & Newsome, W.T. Cortical microstimulation influences perceptual judgements of motion direction. *Nature* **346**, 174–177 (1990).
4. Shepherd, G.M., Pologruto, T.A. & Svoboda, K. Circuit analysis of experience-dependent plasticity in the developing rat barrel cortex. *Neuron* **38**, 277–289 (2003).
5. Pettit, D.L., Helms, M.C., Lee, P., Augustine, G.J. & Hall, W.C. Local excitatory circuits in the intermediate gray layer of the superior colliculus. *J. Neurophysiol.* **81**, 1424–1427 (1999).
6. Yoshimura, Y., Dantzker, J.L. & Callaway, E.M. Excitatory cortical neurons form fine-scale functional networks. *Nature* **433**, 868–873 (2005).
7. Dalva, M.B. & Katz, L.C. Rearrangements of synaptic connections in visual cortex revealed by laser photostimulation. *Science* **265**, 255–258 (1994).
8. Lima, S.Q. & Miesenbock, G. Remote control of behavior through genetically targeted photostimulation of neurons. *Cell* **121**, 141–152 (2005).
9. Banghart, M., Borges, K., Isacoff, E., Trauner, D. & Kramer, R.H. Light-activated ion channels for remote control of neuronal firing. *Nat. Neurosci.* **7**, 1381–1386 (2004).
10. Zemelman, B.V., Nesnas, N., Lee, G.A. & Miesenbock, G. Photochemical gating of heterologous ion channels: remote control over genetically designated populations of neurons. *Proc. Natl. Acad. Sci. USA* **100**, 1352–1357 (2003).
11. Zemelman, B.V., Lee, G.A., Ng, M. & Miesenbock, G. Selective photostimulation of genetically chARGed neurons. *Neuron* **33**, 15–22 (2002).
12. Nagel, G. *et al.* Channelrhodopsin-2, a directly light-gated cation-selective membrane channel. *Proc. Natl. Acad. Sci. USA* **100**, 13940–13945 (2003).
13. Nagel, G. *et al.* Channelrhodopsin-1: a light-gated proton channel in green algae. *Science* **296**, 2395–2398 (2002).
14. Sineshchekov, O.A., Jung, K.H. & Spudich, J.L. Two rhodopsins mediate phototaxis to low- and high-intensity light in *Chlamydomonas reinhardtii*. *Proc. Natl. Acad. Sci. USA* **99**, 8689–8694 (2002).
15. Suzuki, T. *et al.* Archaeal-type rhodopsins in *Chlamydomonas*: model structure and intracellular localization. *Biochem. Biophys. Res. Commun.* **301**, 711–717 (2003).
16. Harz, H. & Hegemann, P. Rhodopsin-regulated calcium currents in *Chlamydomonas*. *Nature* **351**, 489–491 (1991).
17. Mainen, Z.F. & Sejnowski, T.J. Reliability of spike timing in neocortical neurons. *Science* **268**, 1503–1506 (1995).
18. Mermelstein, P.G., Bito, H., Deisseroth, K. & Tsien, R.W. Critical dependence of cAMP response element-binding protein phosphorylation on L-type calcium channels supports a selective response to EPSPs in preference to action potentials. *J. Neurosci.* **20**, 266–273 (2000).
19. Bi, G.Q. & Poo, M.M. Synaptic modifications in cultured hippocampal neurons: dependence on spike timing, synaptic strength, and postsynaptic cell type. *J. Neurosci.* **18**, 10464–10472 (1998).
20. Katz, L.C. & Dalva, M.B. Scanning laser photostimulation: a new approach for analyzing brain circuits. *J. Neurosci. Methods* **54**, 205–218 (1994).
21. Dantzker, J.L. & Callaway, E.M. Laminar sources of synaptic input to cortical inhibitory interneurons and pyramidal neurons. *Nat. Neurosci.* **3**, 701–707 (2000).
22. Schubert, D. *et al.* Layer-specific intracolumnar and transcolumnar functional connectivity of layer V pyramidal cells in rat barrel cortex. *J. Neurosci.* **21**, 3580–3592 (2001).
23. Hirase, H., Nikolenko, V., Goldberg, J.H. & Yuste, R. Multiphoton stimulation of neurons. *J. Neurobiol.* **51**, 237–247 (2002).
24. Ikegaya, Y. *et al.* Synfire chains and cortical songs: temporal modules of cortical activity. *Science* **304**, 559–564 (2004).
25. Kozloski, J., Hamzei-Sichani, F. & Yuste, R. Stereotyped position of local synaptic targets in neocortex. *Science* **293**, 868–872 (2001).
26. Pouille, F. & Scanziani, M. Routing of spike series by dynamic circuits in the hippocampus. *Nature* **429**, 717–723 (2004).
27. Graziano, M.S., Taylor, C.S. & Moore, T. Complex movements evoked by microstimulation of precentral cortex. *Neuron* **34**, 841–851 (2002).
28. Moore, T. & Armstrong, K.M. Selective gating of visual signals by microstimulation of frontal cortex. *Nature* **421**, 370–373 (2003).
29. Deisseroth, K. *et al.* Excitation-neurogenesis coupling in adult neural stem/progenitor cells. *Neuron* **42**, 535–552 (2004).
30. Dull, T. *et al.* A third-generation lentivirus vector with a conditional packaging system. *J. Virol.* **72**, 8463–8471 (1998).